

Impulse-Response Analysis of Toroidal Core Distribution Transformers for Dielectric Design

Pablo Gómez, *Member, IEEE*, Francisco de León, *Senior Member, IEEE*, and Iván A. Hernández, *Student Member, IEEE*

Abstract—Toroidal transformers are currently used only in low-voltage applications. There is no published experience for toroidal transformer design at distribution-level voltages. This paper explores the lightning impulse response of toroidal distribution transformers in order to obtain a dielectric design able to withstand standardized impulse tests. Three-dimensional finite-element simulations are performed to determine the capacitance matrix on a turn-to-turn basis. Then, a lumped parameter RLC model is applied to predict the transient response of the winding as well as to obtain the potential distribution along the winding and corresponding dielectric stresses. The model computes the impulse potential distribution and the dynamic (interturn and interlayer) dielectric stresses. Different insulation design strategies are proposed by means of electrostatic shielding and variation of the interlayer insulation.

Index Terms—Distribution transformers, electrostatic analysis, finite-element method, impulse test, insulation design, toroidal transformers, transient analysis.

I. INTRODUCTION

THERE ARE two basic arrangements for the iron cores presently used to build distribution transformers: 1) core type, where the cores are assembled by stacking laminations and sliding premade coils and 2) shell type, where a continuously wound core is cut and wrapped around the coils a few laminations at a time [1], [2]. In both arrangements, the finished core has air gaps that increase the magnetizing current and the no-load losses.

An alternative construction, currently used for low-voltage applications and explored in this paper for distribution-level voltages, is to use a core made of a continuous steel strip shaped like a doughnut (toroid) with the coils wound around [3]; see Fig. 1. This gapless construction allows for the construction of smaller, more efficient, lighter, and cooler transformers [4], [5].

Manuscript received July 09, 2010; revised October 01, 2010; accepted October 05, 2010. Date of publication November 29, 2010; date of current version March 25, 2011. This work was supported by the U.S. Department of Energy under Grant DEOE0000072. Paper no. TPWRD-00522-2010.

P. Gómez is with the Electrical Engineering Department of SEPI-ESIME Zacatenco, Instituto Politécnico Nacional (IPN), U. P. Adolfo López Mateos, Mexico City 07738, Mexico (e-mail: pgomez@ipn.mx).

F. de León is with the Department of Electrical and Computer Engineering, Polytechnic Institute of New York University, Brooklyn, NY 11201 USA (e-mail: fdeleon@poly.edu).

I. Hernandez is with CINVESTAV Guadalajara, Jalisco 45015, México (e-mail: ihernand@gdl.cinvestav.mx).

Color versions of one or more of the figures in this paper are available online at <http://ieeexplore.ieee.org>.

Digital Object Identifier 10.1109/TPWRD.2010.2087043

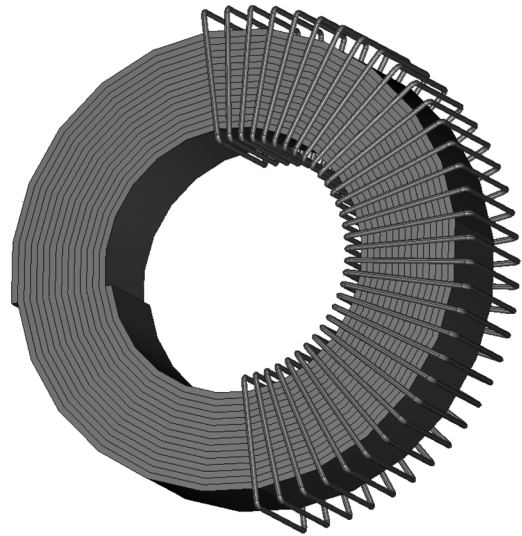


Fig. 1. Toroidal transformer (only a few turns of one winding are shown).

The no-load losses are substantially reduced. There are also savings in the load losses because the windings have fewer turns since these transformers can be designed with a larger flux density. Therefore, there are savings in raw materials (iron and copper) for the same losses than a standard design and even the tank is smaller.

This work is part of a project supported by the U.S. Department of Energy aimed to benefit from the toroidal construction virtues to construct and install toroidal transformers suitable for power distribution application. Given the lack of experience with this type of design at medium and high voltages, studies including electromagnetic, thermal, and mechanical analysis are required to understand its particular physical behavior. This paper is part of a series describing such studies via computational design, optimization, and verification, building prototypes, performance verification, and observation of prototypes installed on a utility distribution system.

This paper is focused on analyzing the lightning impulse response of a toroidal distribution transformer in order to obtain a dielectric design able to withstand standardized impulse tests. This is done by means of three-dimensional (3-D) finite-element simulations, as well as electromagnetic transient simulations considering a lumped parameter RLC (turn-by-turn) model of the transformer winding. These computational tools, which have been extensively used for electromagnetic transient analysis of conventional transformer arrangements (see, for instance, [6]–[11]) are applied in this paper for toroidal distribution transformers for the first time.

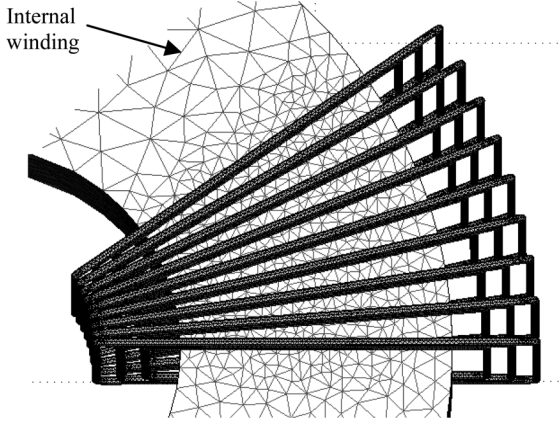


Fig. 2. Geometry and meshing for FEM simulations (distances between layers were exaggerated for illustration purposes).

Another contribution of this paper is the application of electrostatic shielding in the design of the insulation system of toroidal transformers. Two insulation design strategies are proposed in this paper and their effectiveness in reducing the transient voltage and dielectric stress in the winding is demonstrated. The first one is the addition of an electrostatic shield uniformly spaced with respect to the winding. The second one is the use of an electrostatic shield that has a varying distance to the winding, by means of a gradual increase of insulation thickness between the winding and shield (without affecting the winding positions). The two strategies are equally successful to properly distribute the impulse surge. The selection between them depends on manufacturer efficiencies and preferences.

The dynamic performance of the toroidal transformer insulation system for lightning impulse is studied by means of two examples: one transformer of 25 kVA and another one of 50 kVA. Both transformers have the same ratings in terms of voltage ratio (13.8/0.120 kV) and BIL (95 kV).

II. ELECTROSTATIC ANALYSIS

Given the complex geometry of the windings in a toroidal transformer, a 3-D arrangement is required for the electrostatic analysis, as shown in Fig. 2. In this paper, the internal (low-voltage winding, which is grounded) is represented by a solid toroidal shape since its detailed representation is not needed. Note that the transformer core is not visible. For the purposes of this paper, each turn of the high-voltage winding is modeled as a closed loop, then the mutual capacitances can be obtained from the energy method.

Assuming that the high-voltage winding has N layers and n turns per layer, the following capacitive values need to be computed:

- $C_{s,o}$ self capacitance of any turn at the outer layer (N);
- $C_{s,i}$ self capacitance of any turn at the inner layer (1);
- $C_{s,m}$ self capacitance of any turn at any interior layer ($2, \dots, N-1$);
- $C_{it,o}$ mutual capacitance between any two adjacent turns at the outer layer (N);

- $C_{it,i}$ mutual capacitance between any two adjacent turns at the inner layer (1);
- $C_{it,m}$ mutual capacitance between any two adjacent turns at any interior layer ($2, \dots, N-1$);
- $C_{iL,o}$ mutual capacitance between the i th turn at the outer layer and the i th turn at the following interior layer;
- $C_{iL,m}$ mutual capacitance between the i th turns of any two interior layers.

These elements are computed by means of FEM simulations using the electrostatic energy method [12]. Self capacitances are computed from the electrostatic energy W_i obtained when applying a voltage V_i to the i th turn of the winding

$$W_i = \frac{1}{2} C_{ii} V_i^2. \quad (1)$$

Mutual capacitance C_{ij} is computed from the electrostatic energy W_{ij} obtained when applying voltage at both turns i and j

$$W_{ij} = \frac{1}{2} C_{ij} V_i V_j - \frac{1}{2} (C_{ii} V_i + C_{jj} V_j). \quad (2)$$

Self capacitances must be calculated first from (1) in order to obtain the mutual elements from (2). Mutual capacitances between nonadjacent turns or layers are not considered since FEM simulations have shown that, for the arrangements under study, their values are at least one order of magnitude smaller than the values between adjacent turns. Transient simulations in which capacitive values for all turns (including nonadjacent) were included confirmed that they have no effect on the results for the geometrical configuration under analysis.

An important issue when finding the solution of such a detailed geometry lies in the finite-element meshing. Considering the thin insulation between turns produces very narrow regions. This is particularly true at the internal part of the winding. Therefore, a very large number of elements (in the order of millions) is required to obtain an accurate solution.

Taking advantage of the toroidal symmetry to speed up the simulations and consume less memory, the geometry can be simplified by considering only a section of the actual number of turns and layers. For the example shown in Fig. 2, three layers and nine turns per layer are found sufficient to approximate the capacitance values of a real arrangement of 11 layers with 214 turns per layer. This has been validated by initial simulations in which the results from the complete geometry are compared to those of the simplified one.

Each electrostatic simulation for the calculation of the capacitive matrix takes about 12 min in a powerful computer [two Xeon multicore processors running at 2.27 GHz with 72-GB random-access memory (RAM)].

It can be observed in Fig. 2 that in contrast to shell- or core-type transformers, the distance between turns in a toroidal configuration is not constant. While the distance between turns at the internal part of the toroid is kept at the minimum required to avoid dielectric breakdown, the distance at the external part is several times larger, resulting in small capacitive coupling between turns (series capacitance). Thus, the well-known distribution constant $\alpha = \sqrt{C_{\text{ground}}/C_{\text{series}}}$ is several times

larger for toroidal transformers than that for conventional constructions. This particularity of toroidal transformers produces highly nonuniform initial potential distribution (at the wavefront), giving rise to large dielectric stresses as well as increased transient overvoltages. This makes the use of electrostatic shielding necessary.

III. TRANSIENT ANALYSIS

Fast and very fast front transients in transformers are commonly analyzed using internal models, which can take into account the distribution of the incident surge along the windings. These models are described either by distributed parameters, using the transmission-line theory [13], [14], or as a ladder connection of lumped parameter segments [6], [15]. The latter models can be solved by network analysis or by integrating the corresponding state-space equations.

In addition, an admittance matrix model (black-box model) based on terminal measurements has been presented in [16] and [17]. This model can be implemented in time-domain simulation programs by means of a rational approximation procedure.

For the size of a distribution toroidal transformer and the frequency range involved in the lightning waveform, a turn of the transformer can be considered electrically short. Therefore, a lumped parameter model considering a winding turn as the basic element is chosen in this paper.

This section describes the lumped parameter model used in this paper to obtain the transient response of the winding. It is based in [6] and considers a lossy and frequency-dependent multilayer winding.

After computing the winding capacitance matrix \mathbf{C} , the geometric inductance matrix is obtained as

$$\mathbf{L} = \mu_0 \varepsilon \mathbf{C}^{-1}. \quad (3)$$

In (3), ε is the permittivity of the surrounding medium. Conductor losses due to skin and proximity effects can be computed from the following expression [18]:

$$\mathbf{R} = \frac{1}{d} \sqrt{\frac{2\omega}{\sigma_c \mu_c}} \mathbf{L}. \quad (4)$$

In (4), d is the distance between layers, ω is the angular frequency, σ_c is the conductivity of the winding conductor, and μ_c is its permeability. On the other hand, dielectric losses can be included in the form of a shunt conductance matrix given by

$$\mathbf{G} = (\omega \tan \delta) \mathbf{C} \quad (5)$$

where $\tan \delta$ is the loss tangent of the winding insulation. From matrices \mathbf{R} , \mathbf{L} and \mathbf{C} , and \mathbf{G} , a nodal system can be defined to describe the winding (Fig. 3)

$$\mathbf{I}(\omega) = \mathbf{Y}(\omega) \mathbf{V}(\omega) \quad (6)$$

where $\mathbf{V}(\omega)$ and $\mathbf{I}(\omega)$ correspond to the vectors of nodal voltages and currents, and $\mathbf{Y}(\omega)$ is the nodal admittance matrix, which is defined as follows:

$$\mathbf{Y}(\omega) = \mathbf{G} + j\omega \mathbf{C} + \mathbf{\Gamma} + \mathbf{G}_{\text{con}}. \quad (7)$$

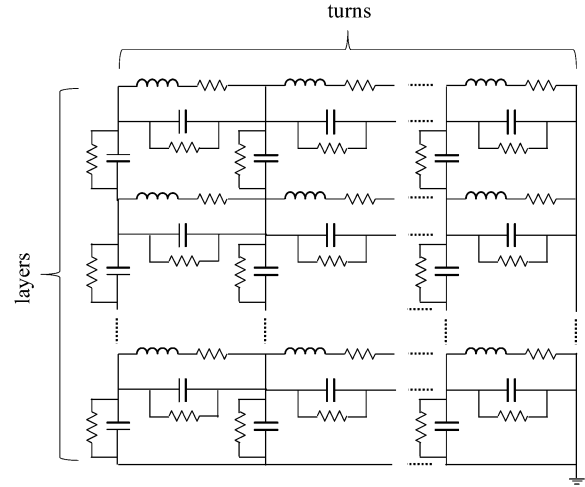


Fig. 3. Circuitual representation of the winding. Mutual inductances between turns and between layers, as well as ground capacitances of outer layers, are omitted in the figure for the sake of simplicity.

Matrix \mathbf{G}_{con} contains the conductance elements required for the topological connection of layers, as well as the source and ground connections (if needed); $\mathbf{\Gamma}$ is the nodal matrix of inverse impedance, computed from $\mathbf{Z} = \mathbf{R} + j\omega \mathbf{L}$ and the incidence matrix \mathbf{K} (since \mathbf{Z} is a branch matrix)

$$\mathbf{\Gamma} = \mathbf{K} \mathbf{Z}^{-1} \mathbf{K}^t \quad (8)$$

where

$$\mathbf{K} = \begin{bmatrix} 1 & 0 & 0 & \dots & 0 & 0 \\ -1 & 1 & 0 & \dots & 0 & 0 \\ 0 & -1 & 1 & \dots & 0 & 0 \\ \vdots & \vdots & \vdots & \ddots & \vdots & \vdots \\ 0 & 0 & 0 & \dots & 1 & 0 \\ 0 & 0 & 0 & \dots & -1 & 1 \end{bmatrix}. \quad (9)$$

Finally, the time-domain response of the winding is obtained by solving (6) for \mathbf{V} and applying the inverse numerical Laplace transform [19], [20].

Maximum dielectric stresses (DS) between turns and between layers can be obtained from the elements of the nodal voltages vector \mathbf{V} and the minimum distance between corresponding turns as

$$\max(\text{DS}_{ij}) = \frac{|V_i - V_j|}{\min(d_{ij})}. \quad (10)$$

IV. ELECTROSTATIC SHIELDING

There are three essential methods to improve the impulse response of power transformers: 1) electrostatic shielding; 2) addition of dummy strands; and 3) interleaving of turns [1]. The latter method is, in general, preferred for transformers working at high-voltage transmission levels. However, for a toroidal transformer working at the distribution-level voltage with a large turns ratio (e.g., 13.8/0.120 kV), the winding arrangement (by layers) and the small cross-sectional area of the winding

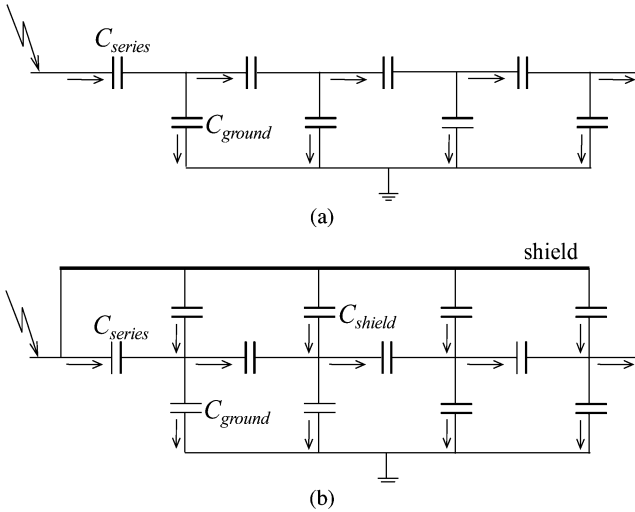


Fig. 4. Initial current distribution along the winding. (a) Original. (b) With the electrostatic shield.

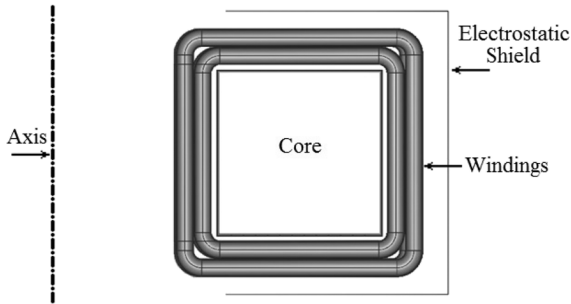


Fig. 5. Axisymmetric view of the toroidal transformer with an inverted C-shape electrostatic shield.

conductors makes it cumbersome and ineffective to attempt any interleaving or addition of dummy strands.

Hence, electrostatic shielding is chosen for toroidal distribution transformers. Its basic idea is to improve the initial potential distribution by compensating the current drained by the ground capacitances with currents injected to the series capacitances [20]. This is illustrated in Fig. 4. The shield is connected to the winding terminal and, therefore, it needs to be isolated from the turns and the tank along its length. Also, the shield should not form a closed path; a gap between the shield ends is necessary.

An electrostatic shield, inverted C-shaped, is proposed for the toroidal transformer constructed by means of a thin conductor material covered by an insulation layer and partially wrapped around the winding. The internal part of the winding remains unshielded (unwrapped) since the turns are close enough to each other in this region; see Fig. 5. In addition, note that the size (and, therefore, the cost) of the toroidal transformer is very much dependent on the minimum internal diameter needed for the winding machine. Therefore, not shielding the center is convenient.

The distance between the shield and the winding is of particular importance. The shield has to be close enough to the winding to be effective and far enough from the winding to avoid dielectric breakdown. This is analyzed for the test case presented the next section.

TABLE I
MAIN GEOMETRICAL DATA OF THE TRANSFORMERS UNDER STUDY

Rating [kVA]	25	50
External diameter of the core [mm]	510	600
Internal diameter of the core [mm]	250	250
Conductor gauge [AWG]	11	7
Conductor diameter [mm]	2.3048	3.6648
Distance between layers [mm]	1.0762	1.0940
Distance between windings [mm]	1.0000	1.0000
Distance between winding and core [mm]	1.0000	1.0000
Minimum distance between turns [mm]	0.0762	0.0940
Number of layers	11	12
Number of turns per layer	214	108

V. TEST CASES

Two toroidal transformers with a rating of 25 and 50 kVA are considered. The voltage ratio and BIL rating are the same for both: 13.8/0.120 kV and 95 kV. The main geometrical data of the high-voltage windings of these two transformers are listed in Table I. The following assumptions are made for simulation purposes:

- The number of turns is considered equal for all layers; in an actual transformer, each outer layer has fewer turns than the previous one.
- Due to the previous assumption, turns from each layer are considered completely aligned, as shown in Fig. 2.
- The minimum distance between turns is given by the typical thickness of the varnish film for the corresponding conductor diameter [22].
- The distance between layers is initially assumed to be 1 mm (plus the conductor varnish).

The set of capacitive values obtained from FEM for both transformers is listed in Table III. An alternating direction of the winding between layers is proposed (i.e., if the first layer is wound in the clockwise direction, then the 2nd layer is wound in the counterclockwise direction and so forth). This winding strategy yields reduced dielectric stresses when compared with continuous (same direction) windings.

The transient response of the transformers is analyzed by means of the injection of a standard 1.2/50- μ s lightning impulse (full wave) at the initial terminal of the winding, which is located at the outermost layer of the winding. The lumped parameter model shown in Fig. 3 is constructed and solved as described in Section III.

The performance of the shield is improved by a configuration equivalent to gradually removing the shield from the winding, which helps to approximate a uniform potential distribution. This is possible by: 1) decreasing the shield surface or 2) increasing the distance between the winding and the shield. However, option 1) implies a constant distance between the shield and the winding, which could result in a dielectric breakdown since the initial potential along the winding drops rapidly while the potential in the shield remains almost constant.

After substantial simulation tests, three alternatives of electrostatic shielding are deemed to be practical: two shields with constant distances of 1 and 2 mm to the outer layer of the

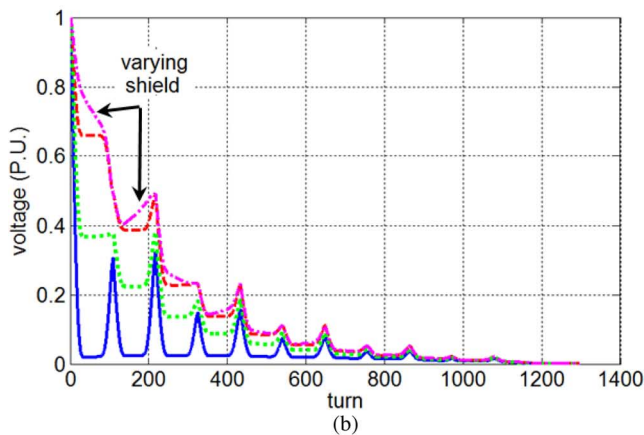
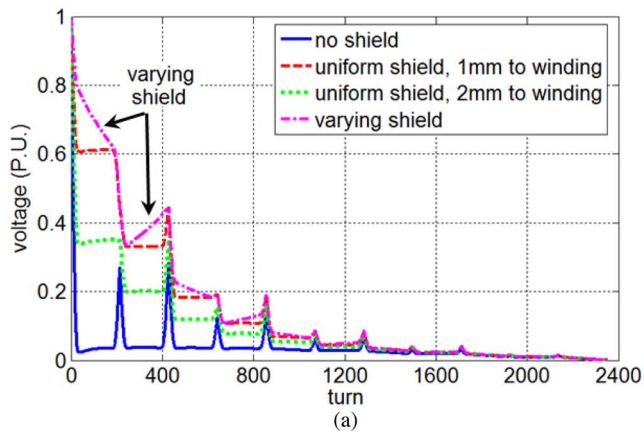


Fig. 6. Initial potential distribution. (a) 25-kVA transformer. (b) 50-kVA transformer.

winding as well as a shield with a varying distance to the outer layer, from 0.1 mm to 1 mm. The latter shield is included by means of gradually increasing the insulation thickness between the winding and shield.

Fig. 6 shows the initial potential distribution along the windings. As expected, the potential distribution without shield (continuous line) is highly nonuniform for both transformers. In addition, some spikes can be seen, which are a consequence of the capacitive coupling between layers at the layers' ends. This distribution can be improved by including an electrostatic shield in the transformer design.

The way in which the different shields affect the initial potential distribution is shown in Fig. 6. By producing a more uniform distribution, the voltage drop between consecutive turns along the winding is reduced.

Fig. 7 shows the transient response of the winding at turn 107 for the 25-kVA transformer and at turn 52 for the 50-kVA transformer, corresponding to the regions of maximum voltage stress. One can appreciate that the shield is able to damp the transient oscillations reducing the maximum transient voltages. In addition, as expected, the closer the shield is to the winding, the larger the mitigation of the overvoltage. However, this distance is limited by the dielectric strength of the insulation between winding and shield. The results for the uniform shield distanced 1 mm to the winding and the varying shield are almost identical for both transformers.

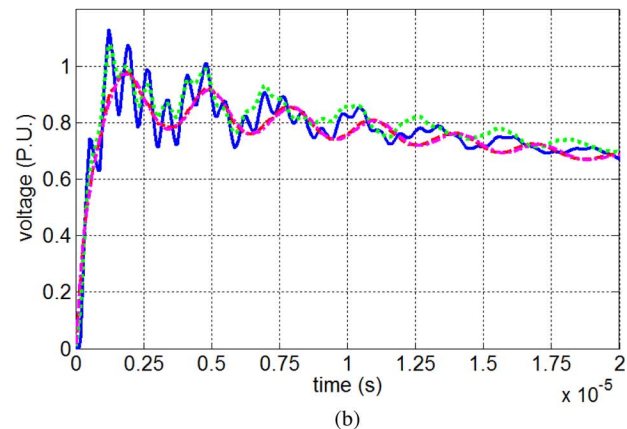
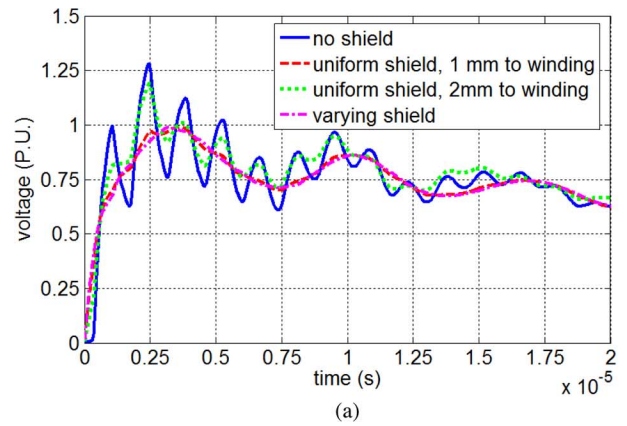


Fig. 7. Transient response at the turn of maximum voltage stress: (a) 25-kVA transformer, turn 107. (b) 50-kVA transformer, turn 52.

Fig. 8 illustrates the distribution of the maximum voltage obtained along the winding for the whole transient period, hereafter called the impulse potential distribution. The voltage distribution along the whole winding of the different shielded transformers is more uniform compared to the unshielded transformers. The performance of the varying shield in the context of mitigating the transient voltage is very similar to that of the uniform shield separated 1 mm from the winding. With these two shielding strategies, the maximum value of the transient voltage is reduced by 21.8% for the 25-kVA transformer, and by 11.3% for the 50-kVA transformer, with respect to the unshielded case.

The dielectric performance of the winding is analyzed considering three main variables:

- 1) interturn dielectric stress;
- 2) interlayer dielectric stress;
- 3) winding-to-shield dielectric stress.

Fig. 9 shows the interturn stress along the complete winding. It can be seen in the plots how the stress is reduced by applying the different shields. The maximum value of interturn stress in the 25-kVA and the 50-kVA transformers is reduced by 57.2% and 56.1%, respectively, with the uniform shield being located 1 mm from the winding. On the other hand, these stresses are reduced by 65.4% and 55.6% with the varying shield. It can also be noticed that even without any shield, the stress is kept to an acceptable level. The maximum value obtained for both transformers is well below the dielectric strength of any high-

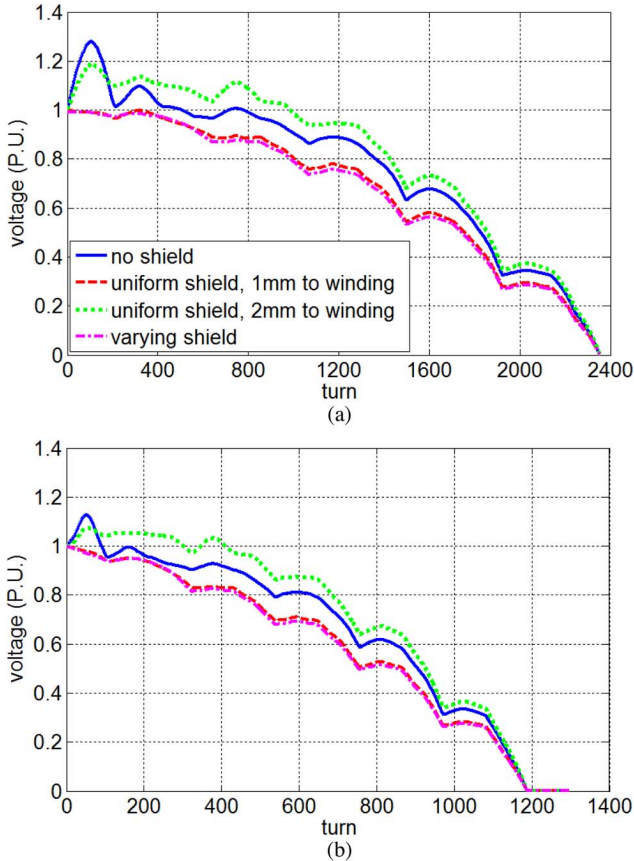


Fig. 8. Impulse potential distribution: (a) 25-kVA transformer. (b) 50-kVA transformer.

performance varnish [17]. Therefore, no extra insulation needs to be added between turns.

The interlayer stress is plotted in Fig. 10. The interlayer stresses are several times larger than the interturn stresses. The potential difference between turns of consecutive layers can be very large, particularly at the layers' ends (corresponding to the peaks in Fig. 9). The stress is especially large between the first two layers for both transformers under analysis. However, the values obtained with or without the shield are below the dielectric strength of a varnish included as reference (56 MV/m) [23].

One can see from Fig. 10 that the shields produce reduced interlayer stresses when compared to the unshielded case. The reduction (in percent) of the stress at each interlayer when applying the shields is shown in Table II. It can be noticed that the reduction is slightly larger when applying the varying shield. Furthermore, the shields produce an increase (by a small percentage) in the stress between layers 1 and 2 for the 50-kVA transformer. This does not present a problem since the stress is still below the dielectric strength of the varnish considered.

From Figs. 8–10, it seems that the best two options are: 1) to use a uniform shield spaced 1 mm from the winding or 2) use a shield with a varying distance to the winding, from 0.1 to 1 mm. Both strategies keep the transient voltage below the BIL, while the interturn and interlayer stresses have acceptable levels.

The performance of the shields in terms of the dielectric stress between the shield itself and the winding is shown in Fig. 11.

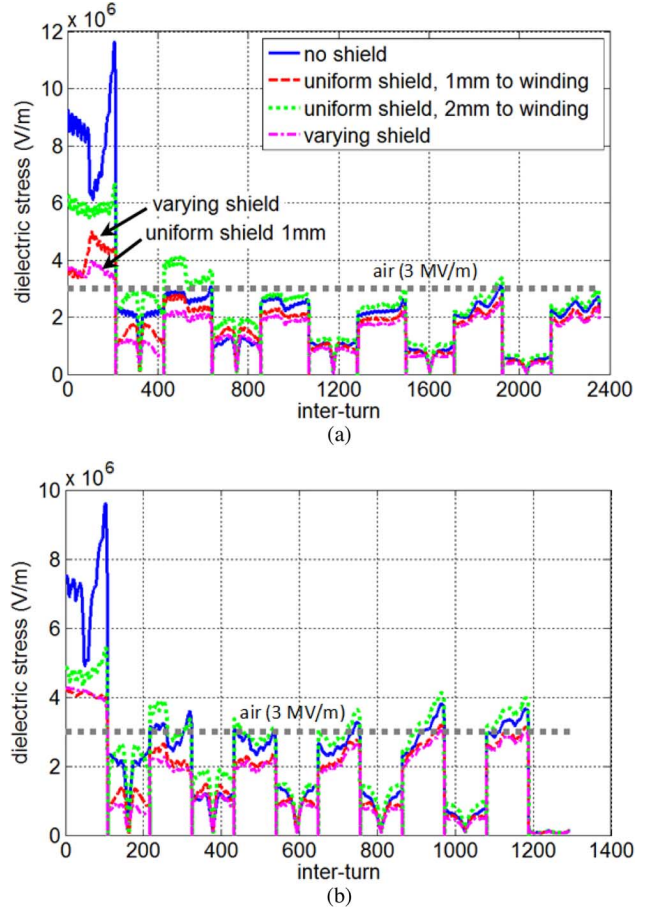


Fig. 9. Interturn dielectric stress. (a) 25-kVA transformer. (b) 50-kVA transformer.

While the uniform shield presents a growing behavior of the stress along the outer layer of the winding, this stress tends to be constant for the varying shield. This means that if the insulation between the winding and the shield is too thin, there is a possibility of dielectric breakdown at the end of the layer when a uniform shield is applied. However, the manufacturing process to include the varying shield is more complicated. Consequently, the uniform shield placed at the correct distance (1 mm for the cases analyzed) can be a better option. All transient voltages and stresses (between turns, layers, and to the shield) are kept at acceptable levels without requiring cumbersome manufacturing of a varying distance of shield to the winding.

VI. CONCLUSION

The dynamic impulse response of a toroidal distribution transformer has been presented in this paper. By means of electrostatic 3-D-FEM simulations, the turn-by-turn capacitance matrix of the winding has been computed. Transient simulations on a lumped parameter model of the winding are used to design the insulation. In contrast to conventional transformers, the distance between turns in a toroidal core transformer is not constant. The larger distance between turns at the external region of the toroidal core yields a smaller series capacitance compared with traditional designs producing a very nonuniform initial potential distribution. This poses stringent

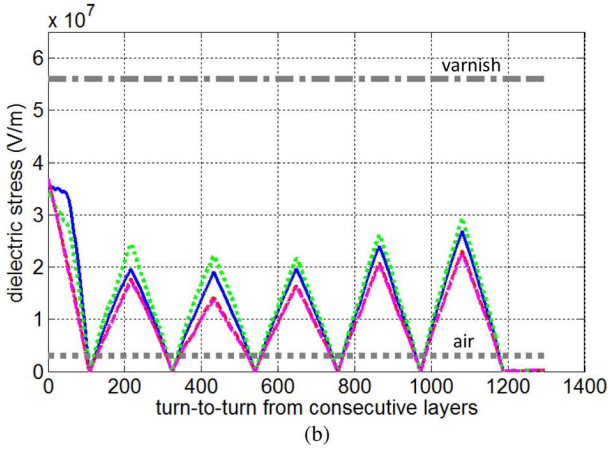
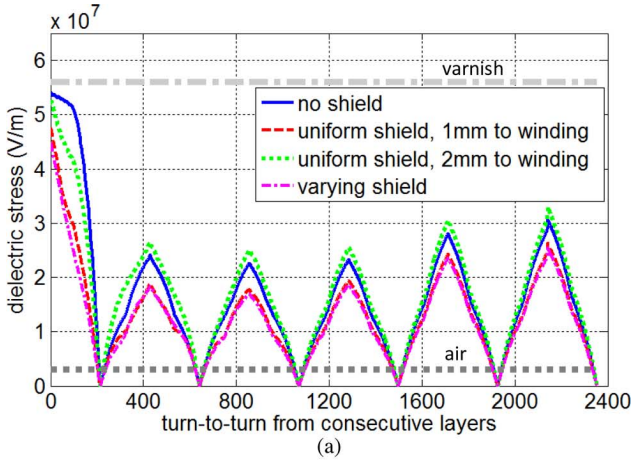


Fig. 10. Interlayer dielectric stress. (a) 25-kVA transformer. (b) 50-kVA transformer.

TABLE II
REDUCTION OF THE INTERLAYER STRESS WITH APPLICATION OF THE ELECTROSTATIC SHIELDING

Inter-layer	Dielectric stress reduction (%)			
	Uniform shield		Varying shield	
	25 kVA	50 kVA	25 kVA	50 kVA
1-2	12.0	-3.9*	17.0	-5.1*
2-3, 3-4	22.3	9.2	23.9	11.2
4-5, 5-6	21.5	25.7	25.1	28.4
6-7, 7-8	16.3	16.3	19.3	18.3
8-9, 9-10	13.5	13.7	16.0	15.8
10-11, 11-12	14.6	14.1	17.0	15.9
HV-LV	14.5	10.2	17.4	16.6

*Negative values correspond to an increase in stress

design constraints since the nonuniform potential distribution gives rise to large transient voltages and dielectric stresses. To overcome this issue, three electrostatic shielding configurations have been proposed: two uniform shields with different distance to the winding and a shield with a linearly increasing distance to the winding. From the results of the simulations performed, the following conclusions are obtained:

- 1) interturn stress is low for the whole winding; atypical insulation film corresponding to its AWG size and a dielectric strength above 12 MV/m is shown to be adequate for the tested cases;

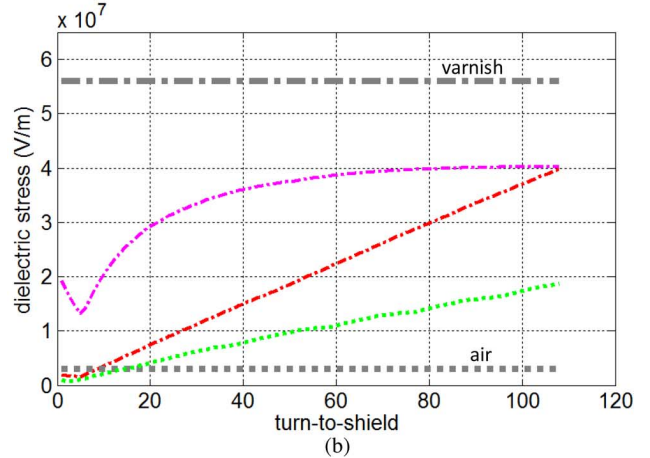
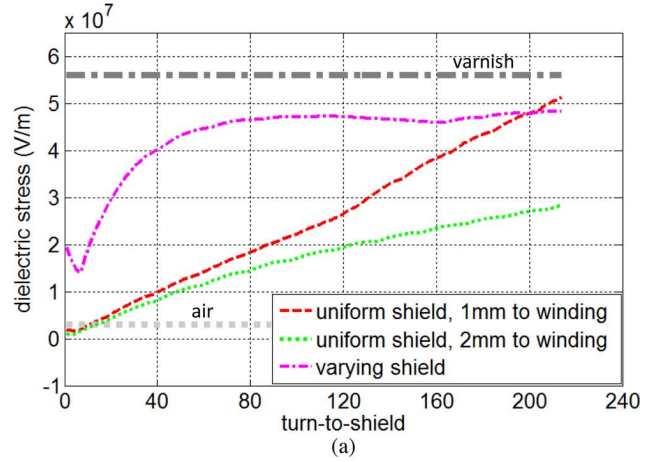


Fig. 11. Winding-to-shield dielectric stress. (a) 25-kVA transformer. (b) 50-kVA transformer.

TABLE III
CAPACITIVE VALUES FOR THE 25-kVA AND 50-kVA TRANSFORMERS WITHOUT SHIELDING

Capacitance*	Value (pF)	
	25 kVA	50 kVA
$C_{s,o}$	71.71	104.32
$C_{s,i}$	56.67	84.23
$C_{s,m}$	63.20	88.70
$C_{il,o}$	25.78	35.23
$C_{il,i}$	10.45	10.90
$C_{il,m}$	15.48	16.44
$C_{il,o}$	13.43	24.76
$C_{il,m}$	12.74	23.24

*Refer to Section II for the corresponding nomenclature

- 2) interlayer stress is the critical factor for these types of transformers; the distance between layers has to be carefully selected to avoid interlayer breakdown;
- 3) the inclusion of a shield at 1 mm from the winding or a shield with a varying distance to the winding (from 0.1 to 1 mm) results in lower interturn and interlayer stress as well as damped transient voltages;
- 4) when a uniform shield is considered, the distance between the shield and winding has to be carefully selected in order to achieve the largest possible reduction in dielectric stress and transient voltage while avoiding dielectric breakdown between the shield and winding;

- 5) this paper proposes a shield with a varying distance to the winding, which prevents dielectric breakdown between the winding and shield.

REFERENCES

- [1] S. V. Kulkarni and S. A. Khaparde, *Transformer Engineering: Design and Practice*. Boca Raton, FL: CRC, 2004, pp. 36–38.
- [2] M. Heathcote, *J&P Transformer Book*. Oxford, U.K.: Newnes, 2007, pp. 13–15.
- [3] I. M. Gottlieb, *Practical Transformer Handbook*. Oxford, U.K.: Newnes, 1998, pp. 12–15.
- [4] G. J. Taggart and J. D. Goff, “Optimizing linear power supply performance with line frequency toroidal transformers,” in *Proc. NorthCon*, Seattle, WA, Oct. 11–13, 1994, pp. 67–71.
- [5] F. de León, B. Gladstone, and M. van der Veen, “Transformer based solutions to power quality problems,” in *Proc. Power Systems World Conf. Exhibit.*, Rosemont, IL, Sep. 2001, pp. 303–314.
- [6] P. I. Fergestad and T. Henriksen, “Transient oscillations in multi-winding transformers,” *IEEE Trans. Power App. Syst.*, vol. PAS-93, no. 2, pp. 500–509, Mar./Apr. 1974.
- [7] Z. Azzouz, A. Foggia, L. Pierrat, and G. Meunier, “3D finite element computation of the high frequency parameters of power transformer windings,” *IEEE Trans. Magn.*, vol. 29, no. 2, pp. 1407–1410, Mar. 1993.
- [8] E. Bjerkan and H. K. Høidalen, “High frequency FEM-based power transformer modeling: Investigation of internal stresses due to network-initiated overvoltages,” presented at the Int. Conf. Power Systems Transients, Montreal, QC, Canada, Jun. 19–23, 2005.
- [9] G. Liang, H. Sun, X. Zhang, and X. Cui, “Modeling of transformer windings under very fast transient overvoltages,” *IEEE Trans. Electromagn. Compat.*, vol. 48, no. 4, pp. 621–627, Nov. 2006.
- [10] F. D. Torre, A. P. Morando, and G. Todeschini, “Three-phase distributed model of high-voltage windings to study internal steep-fronted surge propagation in a straightforward transformer,” *IEEE Trans. Power Del.*, vol. 23, no. 4, pp. 2050–2057, Oct. 2008.
- [11] X. M. Lopez-Fernandez and C. Alvarez-Mariño, “Computation method for transients in power transformers with lossy windings,” *IEEE Trans. Magn.*, vol. 45, no. 3, pp. 1863–1866, Mar. 2009.
- [12] “*AC/DC User’s Guide*,” Comsol Multiphysics, 2006, pp. 1–156, Comsol AB Group.
- [13] Y. Shibuya, S. Fujita, and N. Hosokawa, “Analysis of very fast transient overvoltage in transformer winding,” *Proc. Inst. Elect. Eng., Gen. Transm. Distrib.*, vol. 144, no. 5, Sep. 1997.
- [14] M. Popov, L. V. Sluis, and G. C. Paap, “Computation of very fast transient overvoltages in transformer windings,” *IEEE Trans. Power Del.*, vol. 18, no. 4, pp. 1268–1274, Oct. 2003.
- [15] R. C. Degeneff, W. J. McNutt, W. Neugebauer, J. Panek, M. E. McCallum, and C. C. Honey, “Transformer response to system switching voltage,” *IEEE Trans. Power App. Syst.*, vol. PAS-101, no. 6, pp. 1457–1470, Jun. 1982.
- [16] B. Gustavsen and A. Semlyen, “Application of vector fitting to the state equation representation of transformers for simulation of electromagnetic transients,” *IEEE Trans. Power Del.*, vol. 13, no. 3, pp. 834–842, Jul. 1998.
- [17] B. Gustavsen, “Wide band modeling of power transformers,” *IEEE Trans. Power Del.*, vol. 19, no. 1, pp. 414–422, Jan. 2004.
- [18] K. J. Cornick, B. Filliat, C. Kieny, and W. Muller, “Distribution of very fast transient overvoltages in transformer windings,” 1992, pp. 12–204, CIGRE Rep.
- [19] P. Gómez and F. A. Uribe, “The numerical Laplace transform: An accurate tool for analyzing electromagnetic transients on power system devices,” *Int. J. Elect. Power Energy Syst.*, vol. 31, no. 2–3, pp. 116–123, Feb./Mar. 2009.
- [20] J. Wilcox, “Numerical Laplace transformation and inversion,” *Int. J. Elect. Enging. Educ.*, vol. 15, pp. 247–265, 1978.
- [21] P. Chowdhuri, *Electromagnetic Transients in Power Systems*. Taunton, Somerset, U.K.: Research Studies Press Ltd./Wiley, 1996, pp. 348–351.
- [22] *ANSI/NEMA MW1000-2003 Standard for Magnet Wire*, MW1000, 2003.
- [23] B. Górnicka and L. Górecki, “Method of assessment of varnishes modified with nanofillers,” *Mater. Sci.-Poland*, vol. 27, no. 4/2, 2009.

Pablo Gómez (S’01–M’07) was born in Zapopan, Mexico, in 1978. He received the B.Sc. degree in mechanical and electrical engineering from Universidad Autónoma de Coahuila, Mexico, in 1999, and the M.Sc. and Ph.D. degrees in electrical engineering from CINVESTAV, Guadalajara, Mexico, in 2002 and 2005, respectively.

Since 2005, he has been a Full-Time Professor with the Electrical Engineering Department of SEPI-ESIME Zacatenco, National Polytechnic Institute, Mexico City, Mexico. From 2008 to 2010, he was on postdoctoral leave at the Polytechnic Institute of New York University, Brooklyn, NY. His research interests are in modeling and simulation for electromagnetic transient analysis and electromagnetic compatibility.

Francisco de León (S’86–M’92–SM’02) received the B.Sc. and M.Sc. (Hons.) degrees in electrical engineering from the National Polytechnic Institute, Mexico City, Mexico, in 1983 and 1986, respectively, and the Ph.D. degree from the University of Toronto, Toronto, ON, Canada, in 1992.

He has held several academic positions in Mexico and has worked for the Canadian electric industry. Currently, he is an Associate Professor at the Polytechnic Institute of New York University, Brooklyn, NY. His research interests include the analysis of power definitions under nonsinusoidal conditions, the transient and steady-state analyses of power systems, the thermal rating of cables and transformers, and the calculation of electromagnetic fields applied to machine design and modeling.

Iván Hernández (S’06) was born in Salamanca, Guanajuato, Mexico, in 1979. He received the B.Sc. degree in electrical engineering from the University of Guanajuato, Guanajuato, Mexico, in 2002 and the M.Sc. degree in electrical engineering from the CINVESTAV Guadalajara, Jalisco, Mexico, in 2005, where he is currently pursuing the Ph.D. degree.

From 2008 to 2010, he was a Visiting Researcher at the Polytechnic Institute of New York University. He was an Electrical Engineer Designer for two years with FMS Ingenieria, Guadalajara, Mexico. His research interests are numerical analysis applied to machine design and software simulation tools applied to electromagnetic fields.